

# Enhancing energy performance of glazing systems using solid-solid phase change materials

*Journal of Building Physics*

1–36

© The Author(s) 2025



Article reuse guidelines:

[sagepub.com/journals-permissions](https://sagepub.com/journals-permissions)

DOI: 10.1177/17442591241298952

[journals.sagepub.com/home/jen](https://journals.sagepub.com/home/jen)

Hossein Arasteh<sup>1</sup> , Wahid Maref<sup>1</sup>   
and Hamed H Saber<sup>2</sup> 

## Abstract

In recent years, the implementation of decarbonization measures in response to global warming has brought significant attention to the building sector, recognizing it as a major contributor to CO<sub>2</sub> emissions. This study explores the unique combination of solid-solid phase change material (SSPCM) in double-glazed window (DGW) subjected to different climates, offering a novel approach to enhancing energy efficiency of glazing system, thus Building envelope. To assess the system's energy performance, numerical simulations were performed across a range of temperature conditions. These have included extreme temperatures of the hottest and coldest days of the year, as well as different weather patterns such as sunny and cloudy days in the cities of Montreal, Vancouver, and Miami. The obtained results demonstrated that during summer sunny conditions, energy savings were achieved in both Montreal (17.5%) and Vancouver (23.5%), while Miami experienced energy losses (5.3%). On summer cloudy days, energy savings were observed exclusively in Vancouver (53.6%), whereas energy losses occurred in both Montreal (35.6%) and Miami (36.3%). Under winter sunny conditions, all cities showed energy losses due to the SSPCM blocking beneficial direct solar radiation during the daytime (Montreal: 18.8%, Vancouver: 3.1%, and Miami: 27.0%). Conversely, during winter cloudy conditions, energy savings were noted in all cities, as the SSPCM helped retain warm indoor air (Montreal: 7.0%, Vancouver: 12.4%, and

<sup>1</sup>Department of Construction Engineering, École de Technologie Supérieure (ÉTS), University of Quebec, Montreal, QC, Canada

<sup>2</sup>Deanship of Research and Industrial Development, and Mechanical Engineering Department at Jubail Industrial College, Royal Commission of Jubail and Yanbu, Jubail Industrial City, Saudi Arabia

## Corresponding author:

Hossein Arasteh, Department of Construction Engineering, École de Technologie Supérieure (ÉTS), University of Quebec, 1100, West Notre-Dame Street, Montreal, QC H3C 1K3, Canada.

Email: [hossein.arasteh.1@ens.etsmtl.ca](mailto:hossein.arasteh.1@ens.etsmtl.ca)

Miami: 26.2%). The results revealed that complete visual transparency can be achieved during office hours, enhancing the suitability of the proposed glazing system for commercial applications. These findings can help in designing energy-efficient glazing systems subjected to various climatic conditions.

### **Keywords**

Computational fluid dynamics, carbon-free buildings, phase change materials, fenestration systems, building envelope

## **Introduction**

Over the past years, across both industrialized and developing countries, energy policies in the construction industry have become stringent, with a focus on minimizing energy usage and cutting down carbon dioxide emissions (Zhang et al., 2020). With the rapid pace of urbanization, energy consumption in the construction industry has seen a significant increase over the past decade. While this ongoing expansion is crucial for a country's economic growth and technological progress, it inevitably transforms into a social and environmental challenge, resulting in long-term societal issues (Chen et al., 2019). Despite the limited availability of fossil fuels, global power consumption is projected to rise sharply in the near future. To address the current energy demands, a substantial boost in installed capacity will be essential, and achieving this will require several decades (Loulou and Labriet, 2008). Given these circumstances, governments are increasingly compelled to embrace renewable energy sources and innovative green technologies. This shift is crucial for achieving sustainable growth in all developing sectors (Dodd et al., 2018).

Given that the majority of people spend around 90% of their working time inside and rely extensively on mechanical heating and air conditioning, buildings have emerged as the leading consumers of energy worldwide (Zhao and Magoulès, 2012). Building envelopes serve as the critical interface between indoor and outdoor environments, playing a significant role in mediating the conflicts between occupant comfort and the environmental impact of buildings. Adaptive facades, an advanced component of building envelopes, possess the ability to selectively transmit, filter, or block various phenomena such as heat, mass, and light. This capability enables them to regulate environmental conditions effectively, thereby enhancing indoor environmental quality (Liang and Xiang, 2023). Additionally, adaptive facades offer a promising approach to reducing the energy consumption of buildings. By optimizing the interaction between the interior and exterior environments, adaptive facades contribute to improved indoor comfort and energy efficiency, ultimately supporting the development of more sustainable building practices. Among the opaque and transparent components of building envelopes, the latter is among the building components with the lowest energy efficiency, primarily due to their poor thermal inertia and limited ability to withstand

temperature changes. These systems are responsible for approximately 60% of the overall heat loss, significantly impacting the thermal efficiency of buildings (Badeche, 2022). Moreover, windows allow the majority of solar radiation to pass through, and their use has become increasingly popular among builders and construction firms in recent decades. The widespread adoption of translucent facades in different types of buildings has frequently led to a trade-off between energy efficiency and interior comfort. Problems such as summer overheating, winter energy loss, thermal discomfort, and tenant complaints about glare are common in heavily glazed structures using traditional envelope methods. As a result, there is now considerable research and development aimed at enhancing glazing systems (Truong et al., 2020).

Enhancing the thermal performance of glazing systems in buildings can be achieved through three main strategies namely: (a) improving thermal resistance (Lian et al., 2024; Sun et al., 2024; Xu et al., 2025), (b) implementing solar control (Nur-E-Alam et al., 2024; Yadav and Hachem-Vermette, 2024; Wu et al., 2024), and (c) increasing thermal inertia (Berville et al., 2024; Dellagi et al., 2024; Wagiri et al., 2024; Wang et al., 2023b). The thermal transmittance, which is the reciprocal of thermal resistance of an air-filled space such as enclosed-airspaces in building components (glazing systems in this study), highly depends on several parameters. Due to the heat transfer by natural convection inside the enclosed-airspaces, these parameters include the enclosed-airspace: (a) inclination angle, (b) average temperature, (c) temperature difference, (d) dimensions, and (e) heat-flow directions. For inclined enclosed-airspace, the latter includes heat-flow up to represent the case in which heat leaves the building (cold days), and heat-flow down to represent the case of heat enters the building (hot days). For vertical enclosed-airspace, however, the heat-flow direction is horizontal in which the heat enters building (hot days) or leaves the building (cold days). Several studies were conducted to investigate the effects of these parameters on the thermal resistances of enclosed-airspaces (e.g. see Saber et al., 2024a, 2024b). As an example, for inclined building component having air-filled space at the same values of the parameters (a) through (d), the heat-flow up through the enclosed-airspace results in a higher thermal transmittance in relation to that for heat-flow down. The present study focuses on vertical multi-glazing windows in which the heat flow is horizontal.

In addition, the thermal performance and transmittance of glazing systems can differ based on their orientation and configuration (Tükel et al., 2019). The focus of this study, however, is on improving thermal inertia. This can be accomplished by incorporating thermal energy storage materials, such as phase change materials (PCMs), into the fenestration system. Our recent research has thoroughly reviewed the application of phase change materials (PCMs) in glazing systems, demonstrating their potential to enhance thermal performance, though achieving clear visual quality remains a challenge (Arasteh et al., 2023). PCMs manage heat by absorbing and releasing it through phase change cycles, which can either involve a transition from solid to liquid (solid-liquid phase change materials, SLPCMs) or from one solid state to another (solid-solid phase change materials, SSPCMs).

This study focuses on the use of SSPCMs in glazing systems due to their numerous advantages over SLPCM. SSPCMs exhibit minimal subcooling, reduced material degradation, consistent optical properties, no need for encapsulation, no leakage, less phase segregation, small volume changes, and high thermal stability (Fallahi et al., 2017). Unlike SLPCMs, SSPCMs can be directly applied to a surface or pane of a multi-glazed window, maintaining their solid state throughout the phase transition. This allows the air or inert gas, which has low thermal conductivity, to remain between the indoor and outdoor environments. In contrast, SLPCMs, when filling the air gap, reduce the thermal resistance of the glazing system due to their higher thermal conductivity compared to air. Encapsulation of SLPCMs can mitigate this issue, enabling them to perform similarly to SSPCMs by maintaining a solid phase and preserving thermal resistance. SSPCMs transition between opaque (semi-crystalline) and transparent (amorphous) states, where only the soft segments melt, supported by the hard segments with a significantly higher melting temperature. This ensures that SSPCMs remain solid during phase transitions, with the soft segments melting and freezing while anchored by the hard segments. The phase transition process of SSPCMs has been thoroughly discussed and analyzed in previous studies (Gao et al., 2021).

While there is a wealth of literature on SLPCM applications in glazing units, research on SSPCMs in smart glazing is relatively scarce. Raj et al. (2020) reviewed the applications and recent advancements in the thermophysical properties of SSPCMs, compiling a detailed list of organic, polymeric, organometallic, and commercial SSPCMs, along with their thermophysical properties, phase transition temperatures, melting points, molecular characteristics, and thermal behavior. These reviews are invaluable for researchers and practitioners interested in SSPCM applications. Another review (Fallahi et al., 2017) delved into the molecular properties and thermal characteristics of SSPCMs for thermal energy storage, examining the relationship between molecular structure, phase transition mechanisms, and thermal properties across four main categories: polymeric, organic, organometallic, and inorganic. The authors provided guidance on selecting appropriate SSPCMs for various applications based on desired physical, thermal, and mechanical properties. Gao et al. (2021) integrated a thin SSPCM layer into the interior side of a double-glazing window (DGW) and conducted a numerical analysis to evaluate annual energy savings. Due to limitations in EnergyPlus software for simulating latent energy storage materials, the authors developed an equivalent model. The results indicated that a 3 mm SSPCM layer improved energy savings in warm, mixed, and cold climates, outperforming low-emissivity windows. Wang et al. (2023a) developed an inverse model to derive expressions for the extinction coefficient and refractive index of SSPCMs as a function of temperature for the translucent phase, providing constant values for the opaque and transparent phases. These optical properties were incorporated into the current study. Zhang et al. (2024) conducted a two-dimensional numerical parametric study using the finite volume method to investigate the optical and thermal properties of a triple-glazed window containing SSPCM in the inner air gap and silica aerogel in the outer air gap. The

study simulated 24 h of severe cold weather in a Chinese city. Sensitivity analysis indicated that the thermal efficiency of the glazing system was significantly influenced by the melting temperature and latent heat of the PCM, with the absorption coefficient and refractive index having minor effects. The optimal melting temperature of the PCM was found to be 18°C, resulting in a 15.4% energy saving rate. Guldentops et al. (2018) investigated a building enclosure system using SSPCMs to passively regulate temperature in a south-facing building in central Massachusetts, considering both summer and winter climates. They developed a finite element model to analyze the system's energy performance and identified optimized configurations for each season. However, the study highlighted the need to refine the extinction coefficients and transition temperatures of SSPCMs for effective year-round operation. Ma et al. (2022) assessed a glazing system combining silica aerogel and SSPCM in a severe cold region of China, focusing on both daylighting and energy performance. They used EnergyPlus for energy analysis and Radiance software for daylighting analysis. An equivalent SSPCM model was employed due to software limitations. The study identified transition temperature, latent heat, absorption coefficient, and refractive index as key parameters through sensitivity analysis. A 10 mm thickness of silica aerogel was recommended to maximize energy savings while meeting daylighting standards in China, suggesting the viability of DGW-SSPCM in severe cold regions.

The literature review reveals a lack of studies on the energy performance of SSPCMs in glazing systems using 3D modeling. Existing numerical models often rely on EnergyPlus, which struggles to accurately simulate SSPCM phase transitions, leading to the use of equivalent models. Alternatively, 2D models have been used to evaluate SSPCM behavior when fully occupying the air gap of triple-glazed windows. To address this gap, this study aims to develop a 3D model to assess the energy performance of a double-glazed window (DGW) incorporating SSPCMs. The concept involves placing the SSPCM on the interior pane within the air gap to maintain a high material temperature, ensuring near-complete transparency throughout the year. After validating the model, a parametric study was conducted by varying the transient temperature and temperature range of a south-facing DGW-SSPCM over a 24-h period. Simulations were carried out for both sunny and cloudy conditions on the coldest and hottest days of 2022 in Montreal, Vancouver, and Miami.

## **Research design**

### *Geometric specifications*

This study compares the performance of a double-glazing window with an integrated solid-solid phase change material (DGW-SSPCM) to that of a reference double-glazing window (DGW-REF). The SSPCM is applied to the interior pane within the air gap. Both configurations consist of two panes, each measuring 20 cm by 20 cm with a thickness of 4 mm. The DGW-REF has a 1.6 cm air gap, while the

DGW-SSPCM features a 2 mm-thick SSPCM layer on the interior pane, reducing the air gap to 1.4 cm.

### Thermophysical and optical properties

In this study, the glazing system consists of two clear glass panes, each 4 mm thick, with an emissivity of 0.9 (ASHRAE handbook, 2021). The thermophysical and optical properties of the glass were obtained from (Gowreesunker et al., 2013). The thermal energy storage material (SSPCM) was chosen from (www.pcmproducts.net), and its thermophysical properties were derived from this reference. The optical properties of the SSPCM including refractive index as well as absorption and scattering coefficients were derived from correlations developed by Wang et al. (2023a). Table 1 provides a detailed overview of the thermophysical properties of the materials used in this study. In this study various phase transition temperatures ( $T_c$ ) and phase transition temperature ranges ( $\Delta T_c$ ) are examined. The studied parameters are  $T_c = 20^\circ\text{C}$ ,  $25^\circ\text{C}$ , and  $30^\circ\text{C}$  and  $\Delta T_c = 1^\circ\text{C}$ ,  $3^\circ\text{C}$ , and  $5^\circ\text{C}$  in summer and  $T_c = 10^\circ\text{C}$ ,  $15^\circ\text{C}$ , and  $20^\circ\text{C}$  and  $\Delta T_c = 1^\circ\text{C}$ ,  $3^\circ\text{C}$ , and  $5^\circ\text{C}$  in winter for the SSPCM comparing to the DGW-SSPCM case.

It is important to point out that both  $T_c$  and  $\Delta T_c$  are key characteristics of SSPCMs. In this study, different  $T_c$  and  $\Delta T_c$  values are used to explore how the system behaves under various conditions—whether the SSPCM remains in a transparent phase, remains in an opaque phase, or goes through a full phase change cycle during the day. This approach allows for a comprehensive evaluation of the performance of the system under multiple scenarios. Although different  $T_c$  values are used for summer and winter simulations, this does not necessarily imply that multiple SSPCMs would be required for practical applications. A well-chosen SSPCM with an appropriate  $\Delta T_c$  can potentially accommodate both seasonal variations by managing its phase transition within a suitable temperature range. However,

**Table 1.** Thermophysical properties of the materials utilized in this study.

Property	Air <sup>a</sup>	Glass	SSPCM
Density (kg/m <sup>3</sup> )	1.225	140	1055
Specific heat (J/kgK)	1006.43	840	1630
Thermal conductivity (W/mK)	0.0242	1.3	0.36
Absorption coefficient (1/m)	0	19	25.73 (Transparent) 33.80 (Opaque)
Scattering coefficient (1/m)	0	0	0 (Transparent) 119.02 (Opaque)
Refractive index	1	1.5	1.11 (Transparent) 5.33 (Opaque)
Latent heat (kJ/kg)	–	–	110

<sup>a</sup>Properties at temperature range  $10^\circ\text{C} - 30^\circ\text{C}$ .

careful selection of an SSPCM with an optimized phase transition temperature for specific climates is essential.

The extinction coefficient is defined as the sum of absorption and scattering coefficients (Jin et al., 2022):

$$\sigma_\varepsilon = \sigma_a + \sigma_s \quad (1)$$

The extinction coefficient of a substance, often described by its optical thickness ( $d$ ) as per equation (2), is a standard measure. In this context,  $s$  denotes the actual thickness of the sample, which is 2 mm for the SSPCM-DGW configurations used in this research (ANSYS Inc., 2021).

$$d = (\sigma_a + \sigma_s)s \quad (2)$$

In this study, an isotropic scattering coefficient is assumed. By utilizing Beer-Lambert's law for non-gaseous materials, equation (3) allows for the calculation of PCM transmittance (Guldentops et al., 2018):

$$\tau_{PCM} = 10^{-d} \quad (3)$$

Initially, the absorption coefficient is determined using equation (4; Gowreesunker et al., 2013). This coefficient is subsequently used in equation (1) to calculate the scattering coefficient.

$$\sigma_a = \sigma_s \left[ \frac{\tau_{PCM,tr} - \tau_{PCM,op}}{1 - \tau_{PCM,op}} \beta + \frac{1 - \tau_{PCM,tr}}{1 - \tau_{PCM,op}} \right] \quad (4)$$

For the SSPCM, the refractive index and extinction coefficient are as follows: in the transparent phase, they are 1.11 and  $25.73^{-1}$ , respectively, and in the opaque phase, they are 5.33 and  $152.82^{-1}$ , respectively (Wang et al., 2023a). For the translucent phase, equations (5) and (6) are used to calculate the average optical properties based on the transparency fraction, which replaces the term "liquid fraction" since SSPCM has no liquid phase. The transparency fraction indicates the proportion of the material in the transparent phase, with  $\beta$  being 0 for fully opaque SSPCM and 1 for fully transparent SSPCM. A transparency fraction of 0 means the SSPCM temperature is at or below the lower limit of the transient temperature range, known as the opaque temperature (like the liquidus temperature in SLPCM), indicating the material is in the opaque phase. Conversely, a transparency fraction of 1 means the SSPCM temperature is at or above the upper limit of the transient temperature range, known as the transparentus temperature (like the solidus temperature in SLPCM), indicating the material is in the transparent phase. A transparency fraction between 0 and 1 signifies that the SSPCM is in the translucent phase, akin to the mushy zone in SLPCMs.

$$\sigma_{a,cell} = 33.8\beta + 25.73(1 - \beta) \quad (5)$$

$$\sigma_{s,cell} = 119.02(1 - \beta) \quad (6)$$

where,  $\sigma_{a,cell}$  and  $\sigma_{s,cell}$  represent the absorption and scattering coefficients within a cell of the numerical domain, respectively.

### Governing equations

To model the SSPCM, the enthalpy-porosity approach in FLUENT was used, with a very high viscosity assigned to ensure the material remained nearly stationary. This study focused on evaluating the feasibility and effectiveness of incorporating SSPCM into glazing systems by neglecting natural convection effects within the air gap of the DGW for all configurations (i.e. DGW-SSPCM and DGW-REF). Using the climates of three cities with different conditions (i.e. Montreal, Vancouver, and Miami) as case studies under natural conditions, the approach aimed to determine if energy savings could be realized in a glazing system with SSPCM compared to one without it. The governing equations for this study included the Discrete Ordinates (DO) model for radiation and a solidification/melting model for SSPCM (ANSYS Inc., 2021).

The mass conservation equation is as follows:

$$\frac{\partial \rho}{\partial t} + \nabla \cdot (\rho \vec{v}) = 0 \quad (7)$$

The momentum conservation equation is as follows:

$$\frac{\partial}{\partial t} (\rho \vec{v}) + \nabla \cdot (\rho \vec{v} \vec{v}) = -\nabla p + \nabla \cdot (\mu \nabla \vec{v}) \quad (8)$$

The energy equation is as follows:

$$\frac{\partial}{\partial t} (\rho H) + \nabla \cdot (\rho \vec{v} H) = \nabla \cdot (k \nabla T) + S_h \quad (9)$$

According to equation (9), the enthalpy of the PCM,  $H$ , is determined by adding the sensible enthalpy,  $h_s$ , and the latent heat,  $\Delta H$ , as follows:

$$H = h_s + \Delta H, \quad (10)$$

where,

$$h_s = h_{s,ref} + \int_{T_{ref}}^T c_p dT \quad (11)$$

In equation (10), the fractional latent heat of the PCM,  $\Delta H$ , can be expressed in terms of the PCM's latent heat of fusion,  $L$ . Note that  $\Delta H$  can vary between 0 and  $L$  when  $T_{opaqueus} < T < T_{transparentus}$  (translucent phase).

$$\Delta H = \beta L \quad (12)$$

The transparency fraction can be defined as:

$$\beta = \begin{cases} 0 & \text{if } T \leq T_{\text{opaqueus}} \\ 1 & \text{if } T \geq T_{\text{transparentus}} \\ \frac{T - T_{\text{opaqueus}}}{T_{\text{transparentus}} - T_{\text{opaqueus}}} & \text{if } T_{\text{opaqueus}} < T < T_{\text{transparentus}} \end{cases} \quad (13)$$

The term  $S_h$  in equation (9) denotes the volumetric heat source/sink related to phase change, which is defined as:

$$S_h = - \frac{\partial(\rho\Delta H)}{\partial t} \quad (14)$$

**Radiation equation.** In this study, radiation effects are simulated using the Discrete Ordinates (DO) model, which is the most comprehensive method available in ANSYS FLUENT. This model allows simulation of radiation scattering and absorption across various optical thicknesses. It converts the radiation heat transfer equation into a transport equation for radiation intensity, solving it over a finite number of discrete solid angles (ANSYS Inc., 2021). While this enhances precision, it also increases the number of equations, thereby slowing down the simulation process.

The radiative transfer equation for a medium that absorbs, emits, and scatters at position  $\vec{r}$  in the direction  $\vec{s}$  is given by:

$$\frac{dI(\vec{r}, \vec{s})}{ds} + (\sigma_a + \sigma_s)I(\vec{r}, \vec{s}) = an^2 \frac{\sigma T^4}{\pi} + \frac{\sigma_s}{4\pi} \int_0^{4\pi} I(\vec{r}, \vec{s}') \mathcal{O}(\vec{s}, \vec{s}') d\Omega' \quad (15)$$

The DO model considers the radiative transfer equation in the direction  $\vec{s}$  as a field equation and is written as:

$$\nabla \cdot (I(\vec{r}, \vec{s})\vec{s}) + (\sigma_a + \sigma_s)I(\vec{r}, \vec{s}) = an^2 \frac{\sigma T^4}{\pi} + \frac{\sigma_s}{4\pi} \int_0^{4\pi} I(\vec{r}, \vec{s}') \mathcal{O}(\vec{s}, \vec{s}') d\Omega' \quad (16)$$

In equations (15) and (16),  $\sigma$  is the Stefan-Boltzmann constant ( $5.67 \times 10^{-8}$  W/m<sup>2</sup>K<sup>4</sup>).

### **Climatic conditions**

This study examines a south-facing window glazing system in three cities: Montreal, Vancouver, and Miami. Montreal, located at 45.52°N latitude and 73.42°W longitude, experiences its coldest and hottest days on January 22nd and

July 21st, 2022. The time zone is GMT-5 during Eastern Standard Time (EST) and GMT-4 during Eastern Daylight Time (EDT). Vancouver, situated at 49.3°N latitude and 123.12°W longitude, has its coldest and hottest days on December 22nd and July 29th, 2022. The time zone is GMT-8 during Pacific Standard Time (PST) and GMT-7 during Pacific Daylight Time (PDT). Miami, at 25.76°N latitude and 80.19°W longitude, experiences its coldest and hottest days on January 30th and August 18th, 2022. The time zone is GMT-5 during Eastern Standard Time (EST) and GMT-4 during Eastern Daylight Time (EDT). The study considers all climatic conditions for both sunny and cloudy days on the hottest and coldest days of the year. Ambient weather conditions include hourly wind speed (weatherspark.com), (climate.weather.gc.ca), hourly ambient temperature (weatherspark.com), (climate.weather.gc.ca), hourly solar direct irradiation, and hourly solar diffuse irradiation (ANSYS Inc., 2021), as illustrated in Figure 1.

Montreal, Vancouver, and Miami having Heating Degree Days (HDD) of 4400–4800, 2000–2400, and 0–100, respectively, were selected for the study to represent a diverse range of climate conditions in order to allow for a comprehensive evaluation of the SSPCM's performance in different climatic conditions.

Montreal, which is classified under the Köppen-Geiger climate classification as Dfb (Beck et al., 2018), experiences a humid continental climate with cold winters and warm summers. This climate presents a significant challenge for energy-efficient systems, with extreme temperature variations that test the SSPCM's ability to adapt to both heating and cooling needs. Vancouver, with a Köppen-Geiger classification of Cfb (Beck et al., 2018), has an oceanic climate characterized by mild, wet winters and cool, and dry summers. This relatively moderate climate allows for an evaluation of the SSPCM's performance in a region with less temperature fluctuation compared to Montreal and Miami, providing insights into its effectiveness in milder conditions. Miami's tropical savanna climate, classified as Aw in the Köppen-Geiger system (Beck et al., 2018), features hot, humid summers and warm winters. The city's climate is crucial for assessing the SSPCM's performance in a consistently warm environment, where cooling demands are significant and the material's effectiveness in hot conditions is tested.

### *Initial and boundary conditions*

The initial temperatures for all components in both the DGW-REF and DGW-SSPCM configurations are set to 26°C for summer and 24°C for winter. The window's side surfaces (exterior top, bottom, front, and back) are treated as thermally insulated or adiabatic. Mixed thermal boundary conditions, which include both convection and radiation, are applied to the window's indoor and outdoor surfaces. Therefore, it is necessary to determine parameters such as the heat transfer coefficient, free stream temperature, external emissivity, and external radiation temperature for these surfaces. Furthermore, to account for solar irradiation within the numerical domain, semi-transparent boundary conditions are established. This necessitates defining parameters like direct solar irradiation, diffuse solar

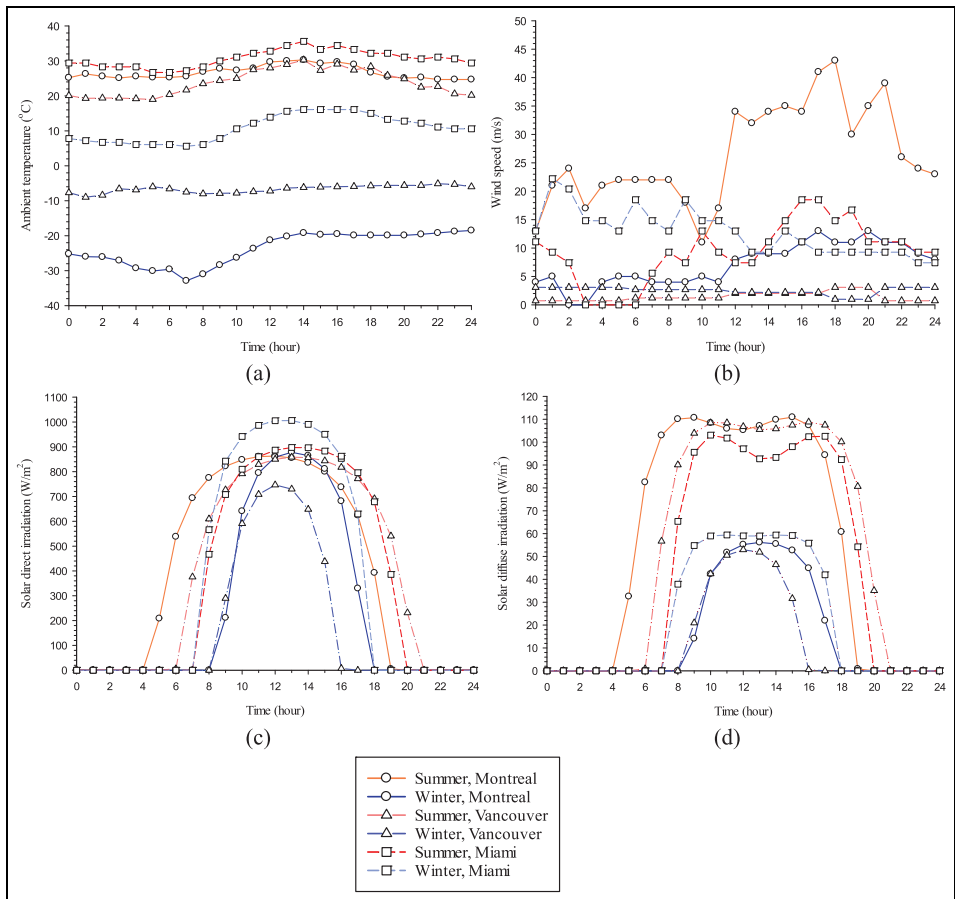


**Figure 1.** Climate data for Montreal, Vancouver, and Miami in summer and winter: (a) Ambient temperature (weatherspark.com and climate.weather.gc.ca), (b) Wind speed (weatherspark.com and climate.weather.gc.ca), (c) Solar direct irradiation (ANSYS FLUENT Theory guide, n.d.), and (d) Solar diffuse irradiation (ANSYS Inc., 2021).

irradiation, and the beam direction vectors in the  $x$ ,  $y$ , and  $z$  directions for both indoor and outdoor surfaces. The emissivity of typical clear glass is set at 0.9 for all boundaries. The sunshine factor is set to 1 to represent a sunny day and to 0 for a cloudy day, which results in zero direct solar irradiation.

The indoor conditions can be determined as a result of conducting numerical simulation for the whole building. However, the present study focuses on assessing the thermal performance of only one building component (double-glazing window) of the building envelope. As such, the indoor conditions are needed as boundary conditions for solving the governing equations. In this study, the heat transfer coefficient for the window's indoor surface thermal and radiation boundary conditions

is set to  $8.7 \text{ W/m}^2\text{K}$  (Jin et al., 2022; Ministry of Housing and Urban-Rural Development, 2016). Both the free stream temperature and the external radiation temperature are set to  $26^\circ\text{C}$  in summer and  $24^\circ\text{C}$  in winter. To avoid modeling direct or diffuse solar irradiation on the indoor surface, no solar irradiation is applied to the indoor radiation boundary condition. As the used indoor conditions above are not the same as those for the case of conducting whole building simulations, the contributions of the windows to the total heating and cooling loads with these indoor conditions may differ from those with the case of conducting whole building simulations. However, the used indoor conditions would insignificantly affect the comparison between the reference double-glazed window without SSPCM and that with SSPCM in terms of the percentages of energy savings/penalties.

To simulate a full 24-h day, the window's outdoor surface thermal and radiation boundary conditions are set using User Defined Functions (UDFs) written in C programming, compatible with the FLUENT library. All parameters except emissivity are imported into ANSYS FLUENT. These UDFs use piecewise linear functions to incorporate hourly weather data. The free stream temperature in the thermal boundary condition is set using the hourly ambient temperature. Additionally, the radiation boundary conditions include hourly values for direct and diffuse solar irradiations and the  $x$ ,  $y$ , and  $z$  beam direction vectors. The hourly heat transfer coefficient, which depends on wind speed, and the hourly external radiation temperature or sky temperature, which depends on ambient temperature, are calculated using equations (17) and (18) (Goia et al., 2012).

$$h_a = 5.62 + 3.9v_{wind} \quad (17)$$

$$T_{sky} = 0.0552T_{air, ambient}^{1.5} \quad (18)$$

## Numerical method

### Model structure and details

The commercial CFD code ANSYS FLUENT (version 2022 R1) is employed, utilizing the SIMPLE algorithm for velocity-pressure coupling. Design Modeler and Ansys Meshing are used to create the geometry and grid, respectively. For pressure, momentum, and energy discretization, a second-order upwind scheme is applied. The DO model and transient formulation use a first-order upwind and first-order implicit scheme, respectively. Convergence criteria are set to be less than  $10^{-6}$  for mass conservation,  $x$ -velocity,  $y$ -velocity, and  $z$ -velocity, and less than  $10^{-9}$  for energy and DO-intensity.

### Numerical validation

This research adapts the model traditionally used for SLPCMs to SSPCMs by employing the solidification/melting model. The primary difference lies in the

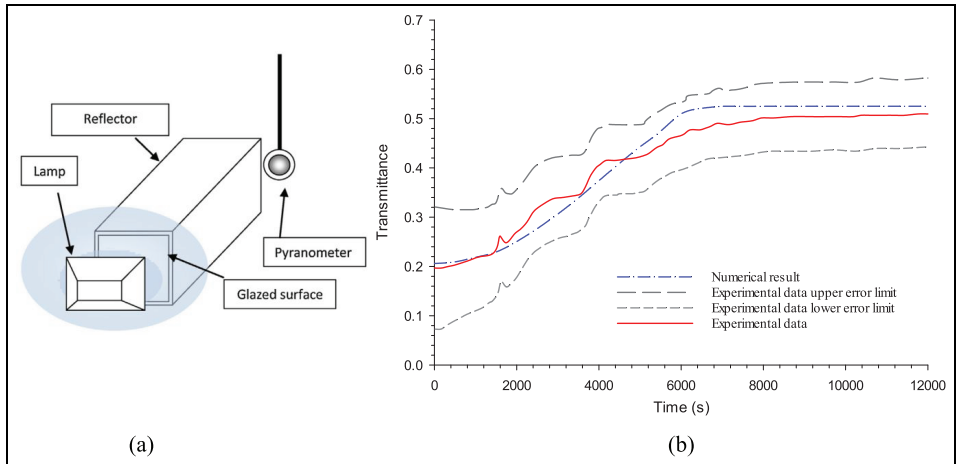


**Figure 2.** (a) A schematic of experimental setup and (b) Current numerical model results compared to the experimental data (Gowreesunker et al., 2013).

absence of natural convection in SSPCMs, as they do not have a liquid phase during melting. By ignoring the gravity effect and considering the high viscosity of the SLPCM's liquid phase, its behavior can be approximated to that of an SSPCM.

To validate the numerical model, which incorporates the Discrete Ordinates (DO) model and the solidification/melting model in glazing systems, researchers compared transient numerical results over a 12,000-second simulation period with experimental data from Gowreesunkera et al. (Gowreesunker et al., 2013) on the transmittance of PCM-filled glazing units over time. They developed an experimental setup, illustrated in Figure 2(a), to measure radiation effects within the mushy phase, which cannot be achieved with a spectrophotometer alone. This setup provided a realistic depiction of radiation behavior in a PCM-glazed system. The entire setup was placed in an environmental chamber with controlled air temperature. A 150 W metal halide lamp emitting diffuse neutral white light was used as the light source. The regular double glazing measured 20 cm by 20 cm with a total thickness of 24 mm, consisting of 4 mm glass, a 16 mm air cavity, and another 4 mm glass layer. In the PCM-filled glazing configuration, the air cavity was replaced with an organic PCM named RT27, produced by RUBITHERM® GmbH. The irradiation level and initial PCM/air temperature were set to  $950 \text{ W/m}^2$  and  $13^\circ\text{C}$ , respectively.

As shown in Figure 2(b), the transmittance values from the simulation align closely with the experimental data, with variations remaining within the margin of error. The overall transmittance was calculated by comparing the radiation flux between the front and back surfaces. The trends observed in the simulation results are similar to those seen in the experimental data. As the numerical results are in agreement with the experimental data being within  $\pm 10\%$  as shown in this figure, the numerical model is validated and can be reliably used in this study.

**Table 2.** Grid sensitivity analysis.

Case	Number of elements	$\overline{q''}$ (W/m <sup>2</sup> )	Error (%)
1	288,923	15.47104	–
2	158,661	15.5293	0.376595
3	82,369	15.58556	0.740245
4	27,440	15.71381	1.569181
5	11,025	15.8746	2.608495
6	4050	16.1296	4.25671

### Grid sensitivity analysis

To achieve a mesh-independent solution, various grid sizes, ranging from fine to coarse, were generated over the numerical domain of a DGW-SSPCM. The criterion for assessing grid independence was the mean total heat flux over a 24-h period on the interior surface of the inner glass pane, as described in equation (19). The results, shown in Table 2, indicate that a grid size with 82,369 elements was approximately optimal, with a relative error of less than 1%. Consequently, this grid size was used in the study.

$$\overline{q''} = \frac{1}{t} \int_0^t q'' dt, \quad (19)$$

where,  $t$  in equation (19) is the time (sec).

### Time step study

The time step sensitivity analysis aims to identify the largest time step that still ensures accurate results. As in the previous section, the method involved calculating the average total heat flux over a 24-h period on the interior side of the inner glass pane to determine the optimal time step, with the goal of minimizing CPU time. The results for various time steps are shown in Table 3, revealing that a 5-min time step produces a relative error of under 1%, making it an appropriate choice for the simulations.

### Energy savings analysis

To comprehensively evaluate the energy savings or losses associated with the DGW-SSPCM system in comparison to the DGW-REF scenario, equation (21) is employed. This equation extends the thermal energy analysis initiated in equation (20). The focus is placed on the average heat flux across the interior surface of the inner pane of the double-glazed window (DGW), denoted as  $\overline{q''}$ , as specified in equation (19). This heat flux can exhibit either a positive or negative value

**Table 3.** Time-step sensitivity analysis.

Case	Time step size	$\overline{q''}$	Error (%)
1	10 s	15.73079	–
2	30 s	15.72085	0.06315
3	1 min	15.70591	0.15812
4	2.5 min	15.66088	0.44443
5	5 min	15.58556	0.92319
6	10 min	15.43214	1.89849
7	20 min	15.11929	3.88729
8	30 min	14.82675	5.74694

depending on its direction: a positive value indicates that heat is moving from the interior of the building to the outside environment, whereas a negative value reflects heat movement from the exterior into the interior of the building.

$$E = \overline{q''} \times t \times A \quad (20)$$

$$\Delta E = E_{final} - E_{ref} \quad (21)$$

Energy savings are realized when the magnitude of the negative heat flux decreases, which suggests a reduction in the amount of heat entering the building. This reduction in heat ingress is crucial for minimizing unwanted heat gain and improving overall energy efficiency. Conversely, energy savings are also achieved when the positive heat flux is reduced, indicating a lower rate of heat loss from the building to the outside. This signifies that less energy is being wasted in maintaining indoor temperatures. By analyzing these changes in heat flux, one can assess the effectiveness of the DGW-SSPCM system in enhancing energy efficiency compared to the DGW-REF scenario, with the ultimate goal of achieving better thermal performance and reduced energy consumption.

## Results and discussion

This section presents a parametric study conducted through numerical simulations over a 24-h period. The analysis focuses on three distinct climatic conditions—Montreal, Vancouver, and Miami—to evaluate the energy performance and thermal behavior of the proposed glazing system. It examines the impact of various parameters, such as phase transition temperature ( $T_c$ ) and its range ( $\Delta T_c$ ), as well as four different weather conditions (summer sunny, summer cloudy, winter sunny, and winter cloudy). The study investigates and analyses how these factors influence the transparency fraction, interior surface temperature, and overall energy savings of the glazing system.

### *Evaluation of optical transmission and transparency characteristics*

Figure 3 illustrates the changes in the transparency fraction of the SSPCM during summer sunny days across the three cities for all cases. As depicted, the transparency fraction exhibits distinct daily patterns at each location, influenced by the phase transition temperature ( $T_c$ ), and the phase transition temperature range ( $\Delta T_c$ ). As temperatures rise, the SSPCM's transparency fraction increases from 0 to 1, reflecting heat storage through its latent thermal energy capacity. Conversely, as temperatures fall, the transparency fraction decreases from 1 to 0, releasing the stored heat. In Miami, the SSPCM maintains full transparency at  $T_c = 20^\circ\text{C}$  and remains fully opaque at  $T_c = 30^\circ\text{C}$  throughout the day. At  $T_c = 25^\circ\text{C}$ , the SSPCM undergoes a full phase transition, staying transparent during office hours. However, due to higher ambient temperatures, Miami experiences longer periods of partial transparency. Larger  $\Delta T_c$  values, such as  $5^\circ\text{C}$  (Figure 3(c)), result in more gradual transitions, while smaller values, like  $1^\circ\text{C}$  (Figure 3(a)), cause sharper changes in transparency. In Vancouver, the SSPCM remains transparent throughout the day at  $T_c = 20^\circ\text{C}$ , but becomes translucent at night with  $\Delta T_c$  values of  $3^\circ\text{C}$  (Figure 3(b)) and  $5^\circ\text{C}$  (Figure 3(c)). At  $T_c = 30^\circ\text{C}$ , partial transitions occur during the hottest part of the day, with the SSPCM returning to opacity by evening. This partial phase transition behavior limits the full utilization of the SSPCM's latent heat storage capabilities. At  $T_c = 25^\circ\text{C}$ , a full transition is achieved, with the SSPCM maintaining transparency during office hours. In Montreal, the transparency fraction rises quickly in the morning, peaks around noon, and declines toward the evening. For  $T_c = 20^\circ\text{C}$ , the transparency remains at 1 throughout the day, ensuring visual clarity. At  $T_c = 30^\circ\text{C}$ , the SSPCM remains opaque with a transparency fraction of 0. At  $T_c = 25^\circ\text{C}$ , a complete phase transition occurs, where smaller  $\Delta T_c$  values (Figure 3(a)) lead to sharper transitions, and larger values (Figure 3(c)) delay the transition. It should be noted that without a full phase transition, the glazing system cannot fully leverage the SSPCM's latent heat storage capabilities. In summary, while Montreal and Vancouver exhibit similar trends, the timing and duration of transitions vary slightly due to climatic differences. The SSPCM's transparency during office hours across all three cities enhances its applicability for commercial uses. In Miami, the consistently warmer conditions lead to extended periods of partial transparency, which may be less critical for visual clarity in offices but still provide adequate daylight for residential buildings.

The SSPCM's transparency fraction behavior over 24 h under summer cloudy conditions is depicted in Figure 4. It is visible that only at  $T_c = 25^\circ\text{C}$  partial phase transition of the SSPCM occurs in all cities, indicating the impact of cloud cover on the SSPCM's performance. The SSPCM's performance in cloudy conditions is characterized by less distinct and lower peaks in transparency fraction compared to sunny conditions, as seen in Figure 3. In Montreal and Vancouver, the full phase transition of the SSPCM does not occur for all scenarios due to the lack of direct solar irradiation, while it occurs in Miami according to higher ambient temperatures. The reduced solar heating on cloudy days limits the SSPCM's ability to fully

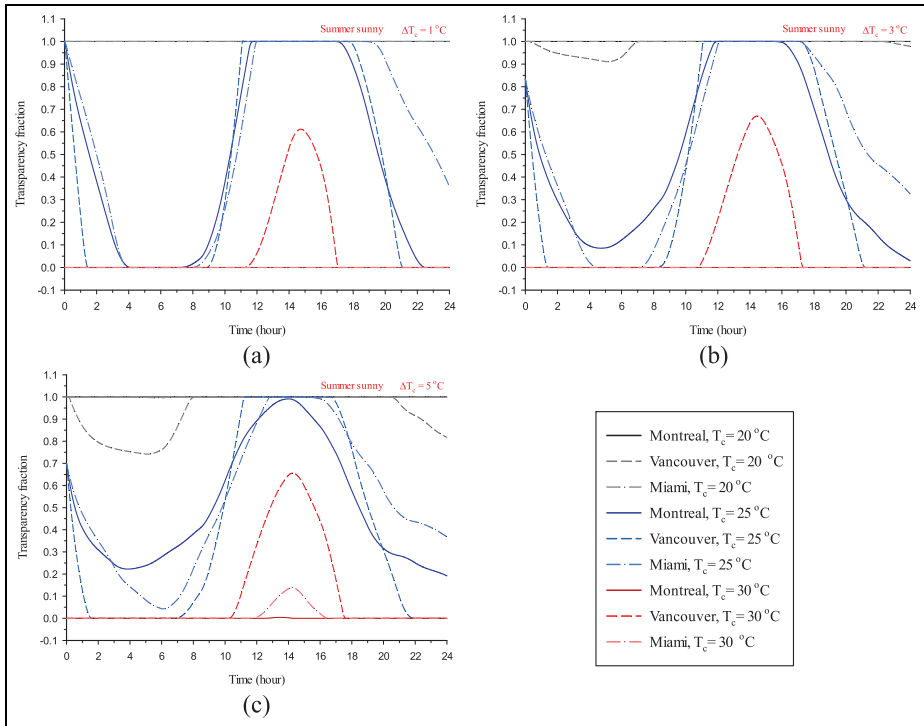


**Figure 3.** SSPCM’s transparency fraction behavior under summer sunny conditions for (a)  $\Delta T_c = 1^\circ\text{C}$ , (b)  $\Delta T_c = 3^\circ\text{C}$ , and (c)  $\Delta T_c = 5^\circ\text{C}$ , across Montreal, Vancouver, and Miami.

transition, thereby impacting its heat storage and release capabilities. Higher  $\Delta T_c$  values (Figure 4(c)) result in more extensive phase transitions of the SSPCM, but these transitions occur more abruptly compared to those with lower  $\Delta T_c$  values (Figure 4(a)). The intermediate  $T_c$  value of  $25^\circ\text{C}$  provides a better balance, ensuring some level of transparency during office hours, enhancing both visual comfort and energy efficiency.

In summer cloudy conditions, in Figure 4, the variation in the transparency fraction of the SSPCM differs across the three cities due to differences in ambient temperatures and solar irradiation. In Montreal and Vancouver, the SSPCM shows minimal or no full phase transition under cloudy conditions because the lack of direct solar irradiation limits its ability to fully transition between transparent and opaque states. This results in a relatively stable but lower transparency fraction, as reduced solar heating diminishes the SSPCM’s heat storage and release capabilities. In contrast, the SSPCM in Miami experiences more noticeable variations in transparency despite the cloudy conditions that resulted in facilitating partial phase transitions even with limited direct solar irradiation. Consequently,

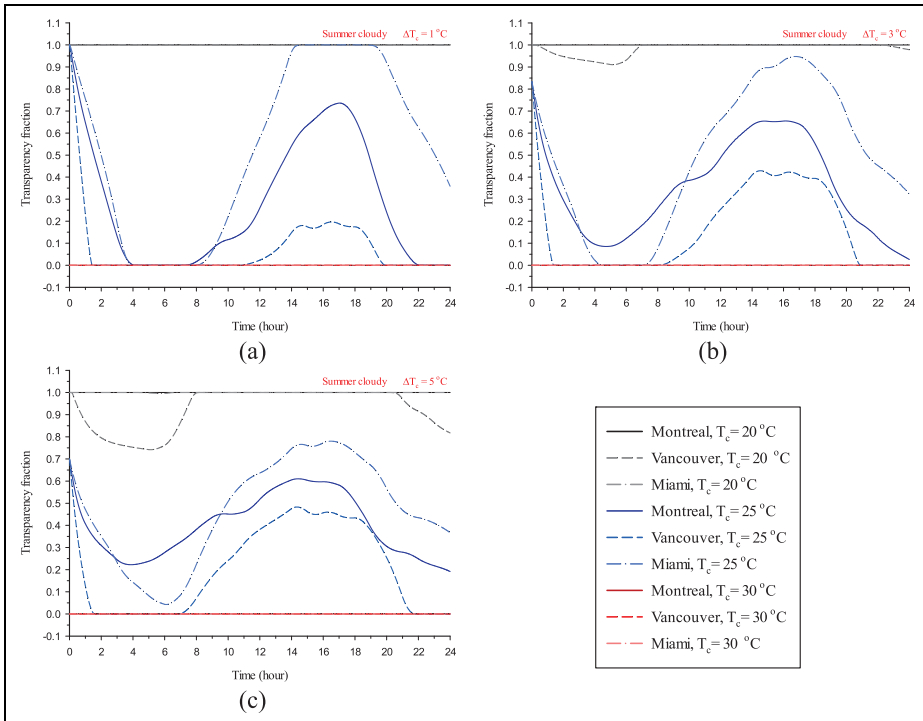


**Figure 4.** SSPCM's transparency fraction behavior under summer cloudy conditions for (a)  $\Delta T_c = 1^\circ\text{C}$ , (b)  $\Delta T_c = 3^\circ\text{C}$ , and (c)  $\Delta T_c = 5^\circ\text{C}$ , across Montreal, Vancouver, and Miami.

Miami's SSPCM exhibits more significant changes in transparency compared to Montreal and Vancouver. The observed differences highlight how ambient temperature and solar irradiation levels influence the SSPCM's performance, with Miami's warmer climate allowing for greater transparency variation under cloudy conditions than the cooler climates of Montreal and Vancouver.

In addition to the differences in transparency fraction observed in various cities, it is also noteworthy that the varying levels of ambient temperature and cloud cover impact the efficiency of the SSPCM in capturing and releasing thermal energy. In cities with higher ambient temperatures like Miami, the SSPCM exhibits a more responsive partial phase transition under cloudy conditions compared to Montreal and Vancouver, which have cooler climates. This indicates that even with limited solar irradiation, the SSPCM can still adapt to temperature fluctuations, albeit less effectively. The performance under cloudy conditions also suggests that in regions with more frequent overcast days, the design of SSPCMs could benefit from incorporating materials with optimized phase transition characteristics or hybrid systems to better handle varying climatic conditions.

Figure 5 illustrates the changes in the transparency fraction of the SSPCM during winter sunny conditions across the three cities studied. In Miami, where winter temperatures are relatively warm, the transparency fraction remains high throughout the day for  $T_c = 10^\circ\text{C}$  and  $T_c = 15^\circ\text{C}$ , indicating consistent transparency. At  $T_c = 20^\circ\text{C}$ , the SSPCM fully transitions, staying opaque at night and transparent during the day, enhancing both visual clarity and thermal storage. In Vancouver, the transparency fraction varies with different  $T_c$  values. For  $T_c = 10^\circ\text{C}$ , transparency remains nearly constant throughout the day. Given Vancouver's milder winter temperatures, the SSPCM remains translucent or transparent at night for  $T_c = 20^\circ\text{C}$  and  $T_c = 15^\circ\text{C}$ , and maintains transparency during the day. This suggests that Vancouver's climate supports a more stable transparency fraction with intermediate  $T_c$  values, balancing visual clarity and thermal storage effectively. In Montreal, the transparency fraction fluctuates significantly throughout the day. With  $T_c$  set at  $10^\circ\text{C}$ , the fraction decreases at night, with greater reductions observed at higher  $\Delta T_c$  values (Figure 5c), causing the SSPCM to become translucent. As the sun rises, it returns to an opaque state. For  $T_c = 20^\circ\text{C}$ , the SSPCM partially transitions from transparent to translucent without fully transitioning. At  $T_c = 25^\circ\text{C}$ , a full phase transition occurs, with  $\Delta T_c$  having a minimal effect on transparency. This configuration allows the SSPCM to remain transparent during office hours and opaque otherwise, making it suitable for commercial buildings. Overall, in winter sunny conditions, the SSPCM effectively manages heat storage and release across all three cities, with noticeable peaks in transparency around midday. The optimal  $T_c$  value for ensuring transparency during key daylight hours while maximizing thermal storage differs by city:  $T_c = 15^\circ\text{C}$  in Montreal, and  $T_c = 20^\circ\text{C}$  in Vancouver and Miami. This highlights the importance of selecting appropriate  $T_c$  values based on local climate to optimize SSPCM performance in double glazing systems.

Figure 6 illustrates the changes in the SSPCM's transparency fraction during winter cloudy conditions across the three cities studied. In contrast to sunny conditions, where transparency peaks are more distinct, the SSPCM displays smaller and less defined transparency peaks on cloudy days, as observed in Figures 3 and 5. The absence of direct solar radiation during cloudy weather restricts the SSPCM's ability to achieve a full phase transition, thus diminishing its effectiveness in heat storage and release. In Miami, the transparency pattern of the SSPCM shows partial transitions, with peaks in transparency occurring later in the day. At  $T_c = 20^\circ\text{C}$ , partial phase transitions are evident and become more pronounced with higher  $\Delta T_c$  values (Figure 6(c)), although the SSPCM remains predominantly opaque throughout the day. In Vancouver, the SSPCM remains mainly translucent throughout the day at  $T_c = 15^\circ\text{C}$ . Lower  $\Delta T_c$  values (Figure 6(a)) lead to greater fluctuations in transparency, reflecting the moderate impact of cloudy conditions on the SSPCM's performance. In Montreal, the SSPCM demonstrates only minor phase transitions, especially at  $T_c = 10^\circ\text{C}$  and with higher  $\Delta T_c$  values. The limited solar radiation results in minimal phase changes, affecting the SSPCM's ability to store and release heat effectively. This comparison between sunny and cloudy

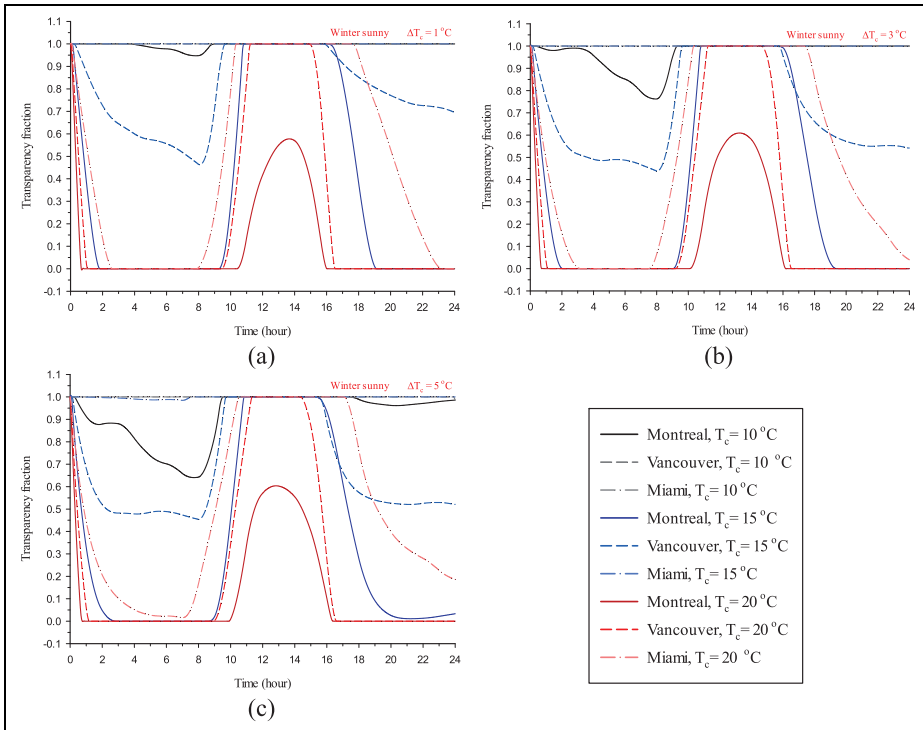
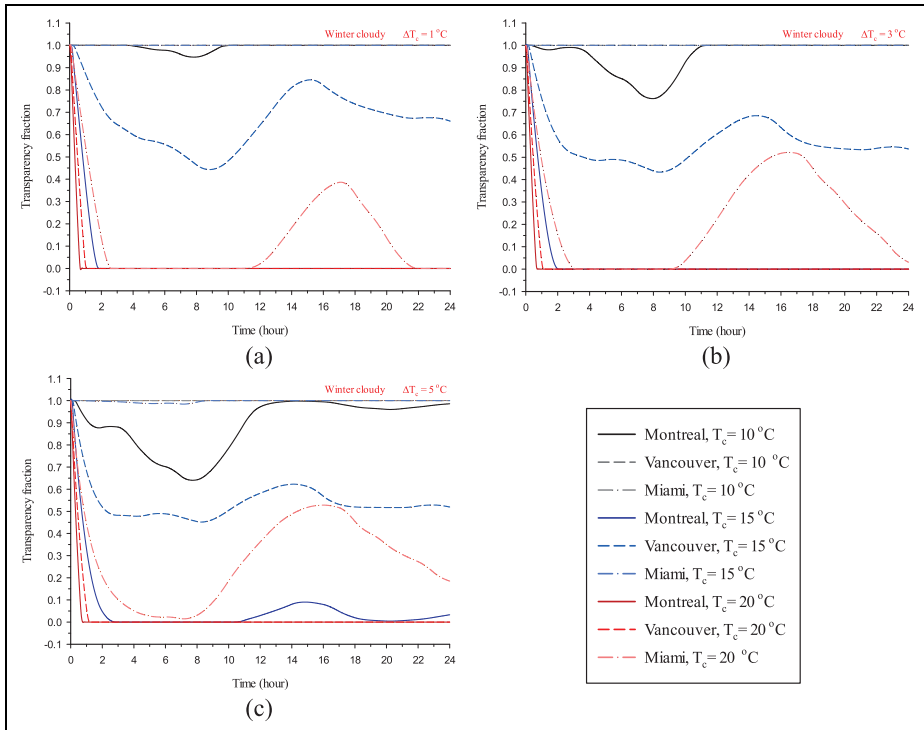


**Figure 5.** SSPCM's transparency fraction behavior under winter sunny conditions for (a)  $\Delta T_c = 1^\circ\text{C}$ , (b)  $\Delta T_c = 3^\circ\text{C}$ , (c) and  $\Delta T_c = 5^\circ\text{C}$ , across Montreal, Vancouver, and Miami.

conditions highlights the importance of considering weather variability when utilizing SSPCMs to achieve optimal energy efficiency and visual comfort.

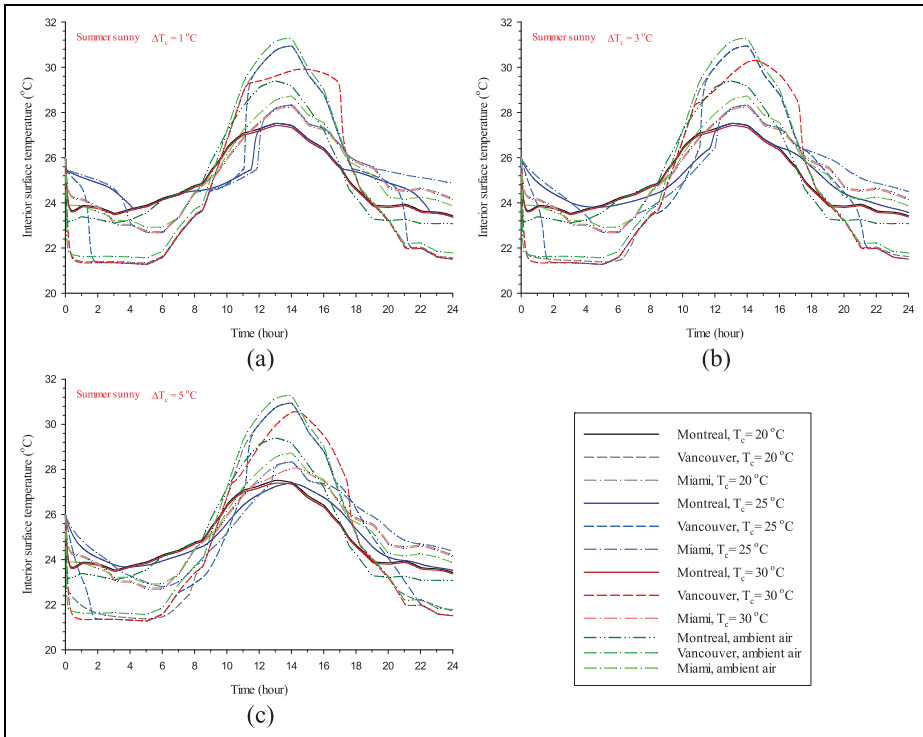
### *Analysis of thermal behavior and temperature profiles on interior surfaces*

Figure 7 illustrates the variations in the interior surface temperature of a double-glazed window equipped with SSPCM under summer sunny conditions across the three studied cities. In Miami, the SSPCM achieves a reduction of approximately  $0.8^\circ\text{C}$  in the interior surface temperature at  $T_c = 30^\circ\text{C}$  and  $\Delta T_c = 1^\circ\text{C}$  (Figure 7(a)) during peak cooling periods. This reduction is attributed to the SSPCM's rapid phase transition, which is facilitated by Miami's consistently warmer climate. The ability of the SSPCM to quickly shift from a transparent to an opaque state helps mitigate heat gains, thus lowering the interior temperature effectively. In Vancouver, the SSPCM results in a slightly lower reduction of around  $0.8^\circ\text{C}$  at  $T_c = 30^\circ\text{C}$  and  $\Delta T_c = 1^\circ\text{C}$  (Figure 7(a)) during peak cooling periods compared to Miami. This reduced cooling effect is due to Vancouver's milder summer



**Figure 6.** SSPCM’s transparency fraction behavior under winter cloudy conditions for (a)  $\Delta T_c = 1^\circ\text{C}$ , (b)  $\Delta T_c = 3^\circ\text{C}$ , and (c)  $\Delta T_c = 5^\circ\text{C}$ , across Montreal, Vancouver, and Miami.

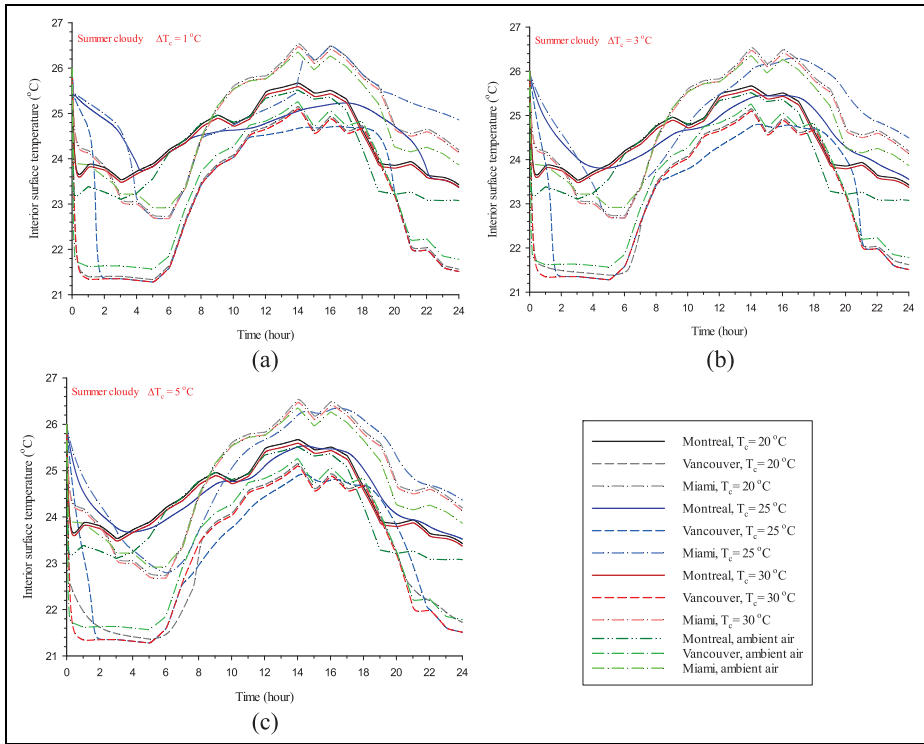
temperatures, which influence the phase transition dynamics of the SSPCM. The SSPCM still provides significant benefits by capturing and storing solar radiation during the day, although the temperature reduction is less pronounced than in Miami. In Montreal, the SSPCM with  $T_c = 25^\circ\text{C}$  and  $\Delta T_c = 5^\circ\text{C}$  (Figure 7(c)) demonstrates a more substantial reduction in interior surface temperature, achieving nearly  $2^\circ\text{C}$  during peak cooling periods. This greater cooling effect is a result of the SSPCM’s high latent heat storage capacity, which efficiently captures and stores solar energy, thus preventing excessive heat from entering the building. During daylight hours, the SSPCM’s ability to maintain a cooler interior is pronounced, while at night, the stored heat is gradually released, causing a rise in temperature. Additionally, lower  $\Delta T_c$  values cause sharper interior surface temperature gradients. Overall, the DGW-SSPCM system exhibits its greatest effectiveness in Montreal’s summer conditions, providing superior thermal comfort by significantly reducing interior temperatures. This underscores the importance of tailoring  $T_c$  and  $\Delta T_c$  values to the local climate to optimize the performance of SSPCMs and enhance summer thermal comfort. Each city’s specific climatic conditions affect



**Figure 7.** Variations of the interior surface temperature of SSPCM under summer sunny conditions for (a)  $\Delta T_c = 1^\circ\text{C}$ , (b)  $\Delta T_c = 3^\circ\text{C}$ , and (c)  $\Delta T_c = 5^\circ\text{C}$ , across Montreal, Vancouver, and Miami.

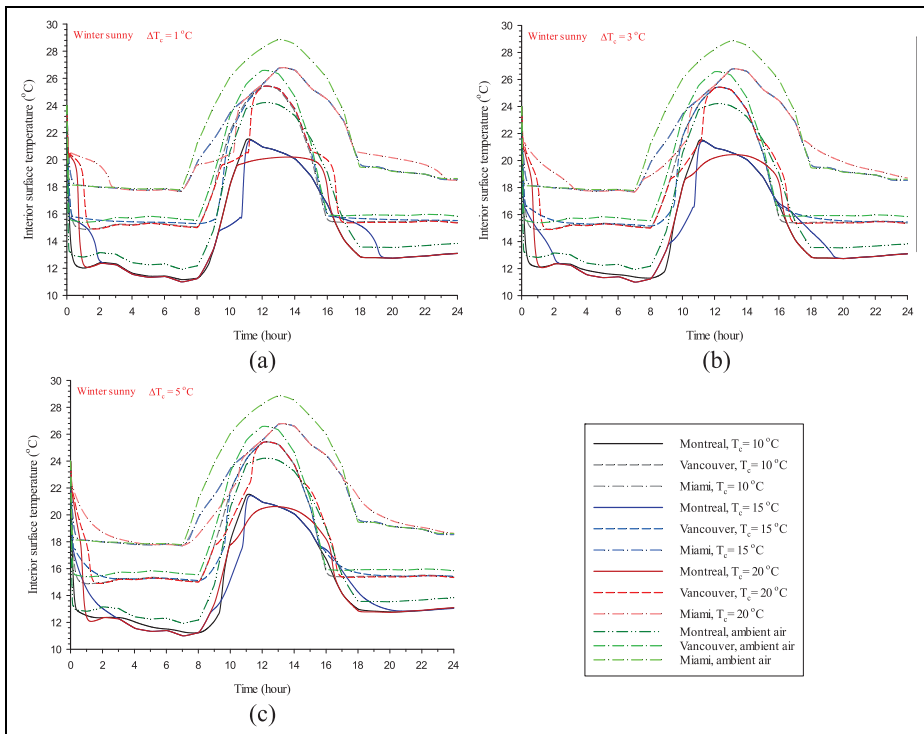
the SSPCM's ability to manage heat gains and losses, highlighting the need for careful selection of system parameters to achieve optimal results.

Figure 8 illustrates the variations in interior surface temperature during summer cloudy conditions across the three studied cities. In Miami, the SSPCM shows a significant reduction in interior surface temperature, maintaining cooler temperatures more effectively due to the warmer climate. The SSPCM's capacity to store heat throughout the day and release it in the evening results in a more noticeable smoothing of temperature fluctuations and improved thermal comfort during peak hours. This highlights the SSPCM's effectiveness in managing temperature variations and reducing cooling loads in Miami's warmer conditions. In Vancouver, the SSPCM also contributes to lowering the interior surface temperature, although the impact is less pronounced compared to Miami. Here, the SSPCM similarly absorbs heat during the day and releases it at night, helping to moderate temperature fluctuations and enhance comfort. The milder summer temperatures in Vancouver result in a less significant reduction in temperature compared to Miami, but the



**Figure 8.** Variations of the interior surface temperature of SSPCM under summer cloudy conditions for (a)  $\Delta T_c = 1^\circ\text{C}$ , (b)  $\Delta T_c = 3^\circ\text{C}$ , and (c)  $\Delta T_c = 5^\circ\text{C}$ , across Montreal, Vancouver, and Miami.

SSPCM still plays a crucial role in stabilizing interior temperatures and improving overall comfort. In Montreal, the SSPCM with  $T_c = 25^\circ\text{C}$  and  $\Delta T_c = 1^\circ\text{C}$  (Figure 8(a)) leads to a reduction of approximately  $1^\circ\text{C}$  in interior surface temperature during peak load hours. The SSPCM’s ability to absorb and store heat throughout the day and release it in the evening helps to moderate temperature swings and improve thermal comfort. Despite the effectiveness of the SSPCM in Montreal, the overall impact on temperature reduction is less compared to Miami, reflecting the colder climate’s influence on the system’s performance. Overall, the DGW-SSPCM system demonstrates its greatest benefit in Miami, where it effectively manages temperature variations and improves thermal comfort during summer cloudy conditions. The system’s performance varies across the cities, with Miami experiencing the most pronounced benefits, followed by Vancouver and Montreal. This variation underscores the importance of selecting appropriate SSPCM parameters to optimize performance based on local climatic conditions.



**Figure 9.** Variations of the interior surface temperature of SSPCM under winter sunny conditions for (a)  $\Delta T_c = 1^\circ\text{C}$ , (b)  $\Delta T_c = 3^\circ\text{C}$ , and (c)  $\Delta T_c = 5^\circ\text{C}$ , across Montreal, Vancouver, and Miami.

Figure 9 presents the variations in the interior surface temperature of the double-glazed window equipped with SSPCM under winter sunny conditions across the three cities studied. In Miami, the SSPCM demonstrates a significant impact on managing heat storage due to the city's warmer winter temperatures. The SSPCM releases stored heat more effectively, causing a notable rise in interior temperature from early evening through midnight. This ability to maintain higher interior temperatures is crucial for comfort during the cooler winter evenings in Miami. In Vancouver, the SSPCM also shows a beneficial effect, though the temperature increase is less pronounced compared to Miami. The milder winter temperatures in Vancouver influence the extent of heat storage and release by the SSPCM. Nevertheless, a notable increase in interior temperature occurs in the early evening at  $T_c = 20^\circ\text{C}$ , highlighting the system's effectiveness in enhancing comfort as heating demands rise. In Montreal, the SSPCM has a significant impact on reducing solar heat ingress during the day. At  $T_c = 15^\circ\text{C}$ , the SSPCM captures and stores heat throughout daylight hours and releases it in the evening, resulting

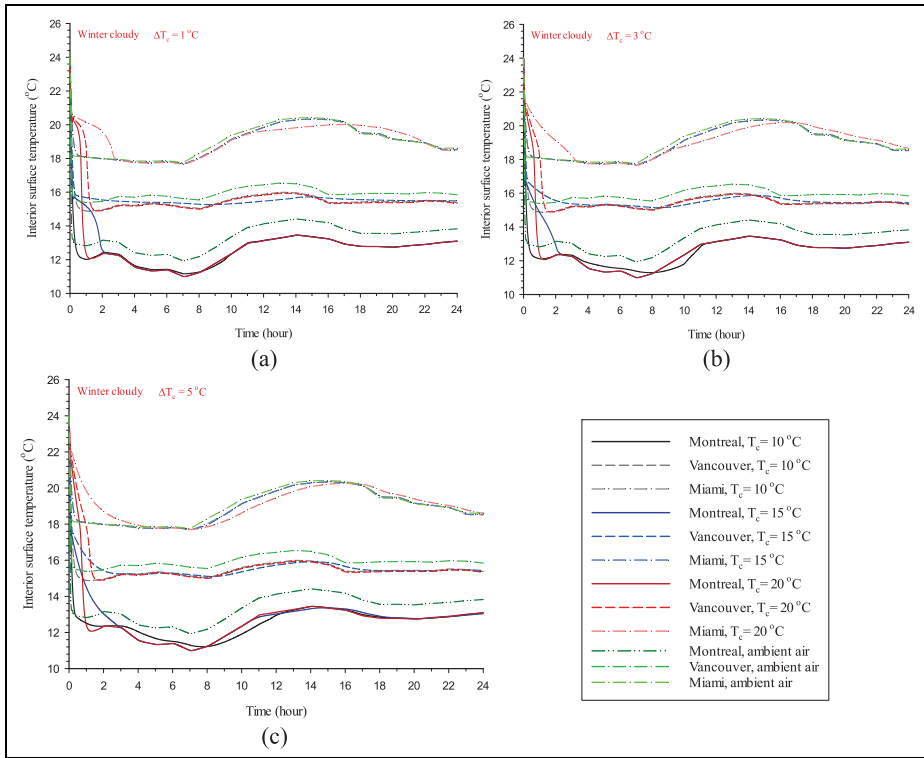


**Figure 10.** Variations of the interior surface temperature of SSPCM under winter cloudy conditions for (a)  $\Delta T_c = 1^\circ\text{C}$ , (b)  $\Delta T_c = 3^\circ\text{C}$ , and (c)  $\Delta T_c = 5^\circ\text{C}$ , across Montreal, Vancouver, and Miami.

in a substantial increase in interior temperature. This effect is particularly noticeable when compared to the DGW-REF system, especially during peak heating periods when the material undergoes a full phase change. The SSPCM thus plays a crucial role in improving thermal comfort in Montreal’s colder winter conditions. Overall, the DGW-SSPCM system proves effective across all studied cities, with each location benefiting from the system’s ability to manage interior surface temperatures based on local winter conditions. In Miami, the system maintains higher interior temperatures effectively, while in Vancouver, it contributes to enhanced comfort in the early evening. In Montreal, the SSPCM significantly improves comfort by managing heat storage and release during peak heating times. These observations emphasize the importance of tailoring SSPCM configurations and  $T_c$  values to optimize performance according to specific climatic conditions.

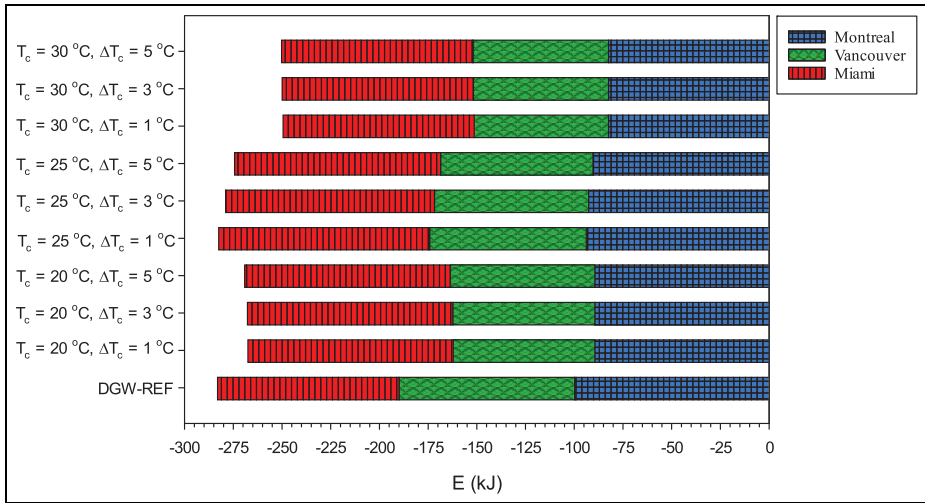
Figure 10 depicts the variations in interior surface temperature for the double-glazed window equipped with SSPCM during winter cloudy conditions across the

three cities studied. Under these conditions, the absence of direct solar radiation significantly affects the SSPCM's ability to manage interior temperatures. In Miami, the SSPCM demonstrates a notable performance even under cloudy conditions due to the city's warmer winter climate. The warmer ambient temperatures allow the SSPCM to complete its phase transition during the day. Consequently, it effectively stores heat and gradually releases it as the outdoor temperatures drop in the evening. This ability to retain and release heat results in increased interior surface temperatures, enhancing thermal comfort during the cooler evening hours. In Vancouver, the SSPCM's performance is less pronounced compared to Miami. The reduced solar radiation during cloudy days limits the SSPCM's capacity to fully engage in its heat storage and release processes. Although the system still manages to store some heat, it does not achieve a full phase transition, leading to less significant improvements in interior temperature regulation and comfort. In Montreal, the SSPCM's effectiveness is notably diminished under cloudy conditions. The lack of direct solar energy prevents the system from undergoing a complete phase change, which is crucial for its thermal management capabilities. As a result, the SSPCM's ability to store and release heat is significantly reduced, leading to less effective temperature regulation and lower thermal comfort. In general, this figure highlights how the SSPCM's performance varies with local climatic conditions during winter cloudy weather. While the system performs relatively well in Miami due to its warmer temperatures, it struggles to maintain effective temperature regulation in colder regions like Vancouver and Montreal. This underscores the importance of considering ambient conditions when assessing the performance of SSPCMs in building applications.

### *Evaluation of energy efficiency: Losses and savings*

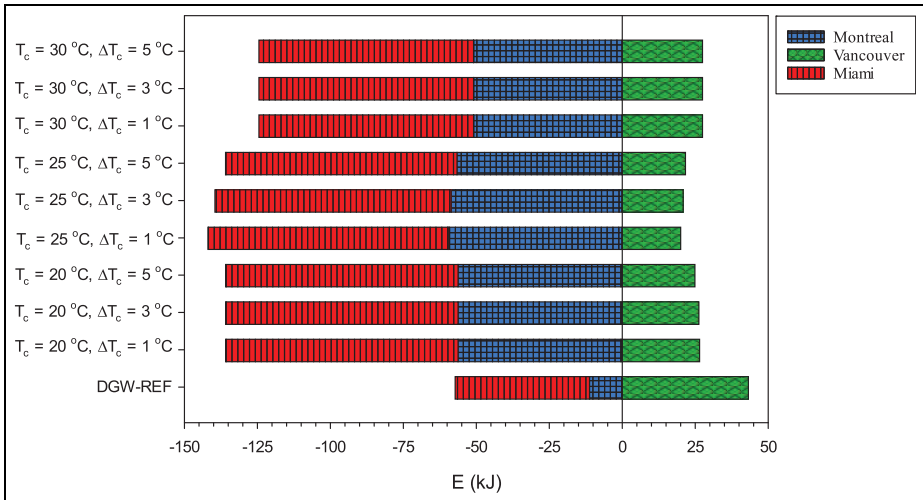
This section provides a detailed assessment of how the proposed glazing system performs in terms of thermal energy across different sky conditions, focusing on three climatically distinct cities: Miami, Vancouver, and Montreal. The performance of the DGW-SSPCM is compared to a DGW-REF system to highlight the impact of the SSPCM under varying temperature conditions.

Figure 11 presents the thermal energy variations for each scenario under summer sunny conditions in these cities, offering a clear visual comparison of the energy performance. In Miami, the energy outcomes for the DGW-SSPCM system differ significantly from those in the other cities. Under Miami's hot and humid summer conditions, the DGW-SSPCM system results in energy losses in all scenarios when compared to the DGW-REF system. This is largely due to the elevated ambient temperatures in Miami, which exceed those found in Vancouver and Montreal, limiting the SSPCM's ability to effectively store and release thermal energy. The energy losses (averaged across the three  $\Delta T_c$ s) for  $T_c = 20^\circ\text{C}$ ,  $25^\circ\text{C}$ , and  $30^\circ\text{C}$  compared to DGW-REF system are 12.2, 13.0, and 5.0 kJ, respectively. The smallest energy losses occur when the SSPCM remains transparent all day at  $T_c = 30^\circ\text{C}$ , as this configuration minimizes heat absorption. However, even with  $T_c$



**Figure II.** The thermal energy performance across three studied cities under summer sunny conditions.

set to  $30^\circ\text{C}$ , the system still underperforms relative to the DGW-REF system due to Miami’s extreme heat, which causes the SSPCM to release stored thermal energy into the building during the night, thereby increasing cooling demands. In Vancouver, the DGW-SSPCM system performs better, demonstrating energy savings across all scenarios compared to the DGW-REF system. The city’s more temperate summer conditions allow the SSPCM to store and release thermal energy more efficiently, making it well-suited to Vancouver’s climate. The energy savings (averaged across the three  $T_c$ s) for  $T_c = 20^\circ\text{C}$ ,  $25^\circ\text{C}$ , and  $30^\circ\text{C}$  compared to DGW-REF system are 16.8, 10.8, and 20.8 kJ, respectively. The highest energy savings occur when  $T_c$  is set at  $30^\circ\text{C}$ , as the SSPCM remains opaque for most of the day, blocking a significant portion of solar radiation. However, the trade-off here is a reduction in visual clarity, which may not be suitable for all building applications. For a balance between energy efficiency and transparency,  $T_c = 20^\circ\text{C}$  offers a more optimal solution, allowing the SSPCM to remain transparent throughout the day while still providing considerable energy savings. This makes the DGW-SSPCM system particularly effective in Vancouver, where the milder temperatures and moderate solar radiation enable the system to optimize its latent heat storage capacity. In Montreal, the DGW-SSPCM system also outperforms the DGW-REF system in terms of energy savings, albeit to a slightly lesser degree compared to Vancouver. Montreal’s climate allows the SSPCM to block solar energy effectively, leveraging its latent thermal storage capability to reduce heat transfer into the building. The energy savings (averaged across the three  $\Delta T_c$ s) for  $T_c = 20^\circ\text{C}$ ,  $25^\circ\text{C}$ , and  $30^\circ\text{C}$  compared to DGW-REF system are 10.4, 7.6, and 17.4 kJ, respectively. The greatest energy savings occur at  $T_c = 30^\circ\text{C}$ , where the SSPCM remains



**Figure 12.** The thermal energy performance across three studied cities under summer cloudy conditions.

opaque, blocking solar radiation and reducing heat gain. However, the lack of visual transparency at this temperature makes it less practical for fenestration systems where visibility is important. For Montreal, the most balanced scenario is when  $T_c$  is set to  $20^\circ\text{C}$ , where the SSPCM remains transparent, ensuring both effective energy savings and clear visibility throughout the day. At  $T_c = 25^\circ\text{C}$ , the SSPCM experiences a full phase transition, but the energy savings are lower than those at  $T_c = 20^\circ\text{C}$  due to the release of stored thermal heat during the nighttime. This release of latent heat back into the interior space results in lower overall energy efficiency, particularly when compared to the  $20^\circ\text{C}$  scenario, where the material stays transparent and maintains a steady thermal performance throughout the day. This analysis underscores the necessity of considering local climatic conditions when designing and implementing SSPCM glazing systems. While the DGW-SSPCM system proves effective in cooler climates like Vancouver and Montreal, it struggles in hotter environments like Miami, where its energy-saving potential is diminished. Tailoring the design of SSPCM systems to the specific thermal demands of each region is crucial to maximizing their effectiveness and ensuring they meet both energy efficiency and functional requirements.

Figure 12 provides a comprehensive view of the thermal energy variations across different scenarios under summer cloudy conditions for the three cities studied—Miami, Vancouver, and Montreal. In Miami, where summer temperatures are consistently high, the absence of direct solar radiation exacerbates the challenges faced by the SSPCM-DGW system. Under cloudy conditions, the SSPCM's ability to store and release thermal energy is diminished, leading to energy losses in all scenarios. In Miami, the energy losses (averaged across the three  $\Delta T_c$ s) for  $T_c = 20^\circ\text{C}$ ,

25°C, and 30°C compared to DGW-REF system are 33.6, 34.9, and 27.5 kJ, respectively. The smallest energy losses occur at  $T_c = 30^\circ\text{C}$ , where the SSPCM remains transparent, minimizing unwanted heat gain or loss. However, even in this optimal scenario, the DGW-SSPCM system is unable to provide energy savings compared to the DGW-REF system, highlighting the limitations of SSPCM technologies in Miami's warm climate, especially under cloudy conditions when the solar energy available for storage is reduced. Similarly, in Montreal, the SSPCM-DGW system also experiences energy losses across all scenarios under cloudy summer conditions, although these losses are generally more pronounced than in Miami. Montreal's comparatively cooler summer temperatures are offset by the absence of direct solar radiation on cloudy days, reducing the effectiveness of the SSPCM. In Montreal, the energy losses (averaged across the three  $\Delta T_c$ s) for  $T_c = 20^\circ\text{C}$ ,  $25^\circ\text{C}$ , and  $30^\circ\text{C}$  compared to DGW-REF system are 45.1, 47.1, and 39.7 kJ, respectively. As in Miami, the smallest energy losses in Montreal occur when  $T_c$  is set at  $30^\circ\text{C}$ , allowing the SSPCM to remain transparent throughout the day, thereby minimizing heat transfer. However, despite this relative improvement, energy losses remain significant under cloudy conditions, demonstrating that the SSPCM-DGW system's performance is highly dependent on the presence of direct solar radiation. The results suggest that while the system offers some advantages under sunny conditions, it struggles to perform optimally in the absence of consistent solar exposure, as is common on cloudy days. In contrast, Vancouver presents a different scenario due to its milder summer climate. Unlike Miami and Montreal, where energy losses are observed across all scenarios, Vancouver's cooler temperatures allow the SSPCM-DGW system to perform more effectively under cloudy conditions. The thermal energy values in Vancouver remain positive, meaning that the SSPCM-DGW system consistently conserves energy by reducing the amount of air-conditioned air lost from the building. In Vancouver, the energy savings (averaged across the three  $\Delta T_c$ s) for  $T_c = 20^\circ\text{C}$ ,  $25^\circ\text{C}$ , and  $30^\circ\text{C}$  compared to DGW-REF system are 17.3, 22.4, and 15.7 kJ, respectively. The highest energy savings occur when  $T_c$  is set at  $25^\circ\text{C}$ , a scenario in which the SSPCM undergoes a partial phase transition, allowing it to optimize its latent heat storage and release capabilities throughout the day. In addition, scenarios where the lowest  $\Delta T_c$  values are employed achieve slightly greater energy savings within the  $T_c = 25^\circ\text{C}$  configuration, although the difference is relatively minor. This trend underscores the importance of the SSPCM's transition temperature,  $T_c$ , in influencing the overall energy performance of the glazing system, with a more pronounced effect than the variation in  $\Delta T_c$ .

Figure 13 presents the thermal energy across all scenarios studied under winter sunny conditions in the three cities. The data indicates that energy losses are observed in every case under these conditions. The energy losses (averaged across the three  $\Delta T_c$ s) for  $T_c = 10^\circ\text{C}$ ,  $15^\circ\text{C}$ , and  $20^\circ\text{C}$  compared to DGW-REF system are 86.4, 66.4, and 64.4 kJ for Montreal; 23.9, 16.8, and 7.1 kJ for Vancouver; and 71.8, 71.8, and 62.0 kJ for Miami, respectively. Across all cities, the data for winter sunny conditions reveal a consistent pattern of energy loss, suggesting that the SSPCM's capacity to block direct solar radiation during the day outweighs the

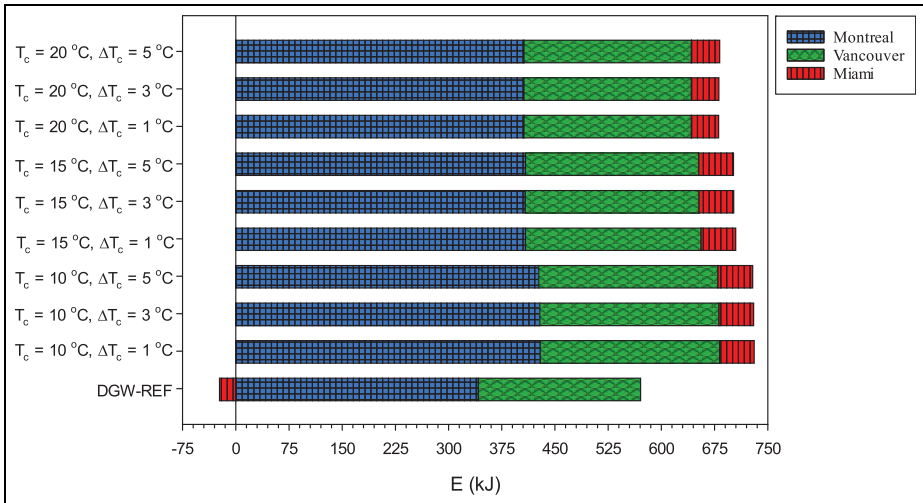


**Figure 13.** The thermal energy performance across three studied cities under winter sunny conditions.

heat it releases into the interior at night, resulting in an overall energy deficit. The scenario with the smallest energy loss is observed when  $T_c = 20^\circ\text{C}$ , where the SSPCM undergoes a phase transition, allowing it to release stored heat at night and maintain transparency for a longer period during the day. Although variations in  $\Delta T_c$  have a minimal effect on energy performance, higher  $\Delta T_c$  values contribute to reduced energy loss due to the extended periods of charging and discharging. Vancouver exhibits lower energy losses compared to Montreal and Miami, likely due to its winter temperatures being intermediate. This highlights the need for tailored designs in glazing systems with thermal energy storage materials, as various parameters significantly impact both energy performance and visual quality.

Figure 14 reveals that under winter cloudy conditions, the fenestration system performs differently, leading to energy savings in all three cities. With no direct solar irradiation, the SSPCM not only releases its stored heat into the indoor environment during the night but also acts as an insulating layer. This helps to retain the warm air inside the building, contributing to the overall energy savings. The energy savings (averaged across the three  $\Delta T_c$ s) for  $T_c = 10^\circ\text{C}$ ,  $15^\circ\text{C}$ , and  $20^\circ\text{C}$  compared to DGW-REF system are as follows: 12.2, 38.9, and 39.3 kJ for Montreal; 30.0, 39.3, and 50.5 kJ for Vancouver; and 42.8, 42.8, and 54.1 kJ for Miami, respectively. The analysis reveals that the highest energy savings occur at  $T_c = 20^\circ\text{C}$  due to the SSPCM’s phase transition throughout the day. Among the cities studied, Miami leads in energy savings, followed by Vancouver, with Montreal ranking third. When comparing the energy saved and lost in the highest-saving scenario, it is evident that in Montreal and Miami, the energy lost on sunny days is nearly 1.7 and 1.2 times greater, respectively, than the energy saved on

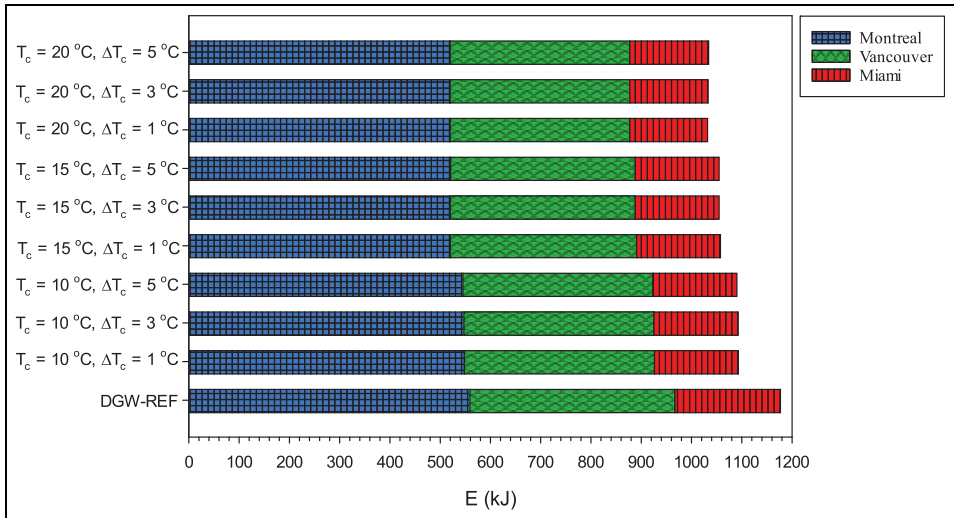


**Figure 14.** The thermal energy performance across three studied cities under winter cloudy conditions.

cloudy days. In contrast, Vancouver experiences a much higher ratio, with energy saved on cloudy days being approximately 7.1 times greater than the energy lost on sunny days. Therefore, the SSPCM-DGW system proves to be most effective in Vancouver during winter for achieving significant energy savings.

### Conclusion

In recent years, the growing urgency to combat global warming has driven substantial efforts toward decarbonization, particularly within the building sector, which is widely recognized as a significant source of CO<sub>2</sub> emissions. As a major contributor to energy consumption and carbon output, the building industry has become a focal point for introducing innovative technologies aimed at improving energy efficiency. One such technology is the integration of solid-solid phase change material (SSPCM) into double-glazed windows (DGWs), which presents a promising solution for reducing energy use in building envelopes. This study investigates the potential of SSPCM-DGW systems in enhancing energy performance across a variety of climates, offering a novel approach to sustainable building design.

The research involved a detailed analysis of the SSPCM’s behavior under varying climate conditions, including extreme temperatures and different weather patterns, to assess its performance across multiple regions. Numerical simulations were conducted to evaluate the system’s effectiveness during both the hottest and coldest days of the year, as well as under both sunny and cloudy conditions. The study focused on three cities with distinct climates: Montreal, Vancouver, and

Miami. These locations were chosen to represent a wide spectrum of temperature variations, allowing for a comprehensive assessment of the SSPCM-DGW system's adaptability to diverse environments.

The results revealed notable differences in energy performance across the three cities. Under sunny summer conditions, the SSPCM-DGW system showed significant energy savings of 17.5% in Montreal and 23.5% in Vancouver, while in Miami, energy losses of 5.3% were recorded. This suggests that the system is more beneficial in cooler or temperate climates where summer solar gains are more manageable. On cloudy summer days, Vancouver was the only city where substantial energy savings were observed, reaching 53.6%. In contrast, both Montreal and Miami experienced energy losses of 35.6% and 36.3%, respectively, indicating that the SSPCM's effectiveness is highly dependent on the weather patterns of each region.

During winter sunny conditions, the system exhibited energy losses across all three cities, as the SSPCM blocked the direct solar radiation that would have otherwise contributed to heating the buildings. The losses were most pronounced in Miami (270%), followed by Montreal (18.8%) and Vancouver (3.1%). However, under winter cloudy conditions, the SSPCM-DGW system performed favorably in all cities. The material's ability to retain indoor heat led to energy savings of 7.0% in Montreal, 12.4% in Vancouver, and 26.2% in Miami. These findings underscore the importance of considering both seasonal and daily weather variations when designing energy-efficient glazing systems.

A particularly noteworthy aspect of this system is its ability to maintain visual clarity during office hours, which makes it an attractive option for commercial buildings. The SSPCM-DGW design allows for complete transparency, ensuring that natural light can enter the building without compromising thermal performance. This dual benefit of energy efficiency and visual transparency is a key feature that enhances the applicability of SSPCM-DGW systems in modern architecture, especially in office and retail spaces where daylighting is a priority.

In general, the influence of the SSPCM's transient temperature on energy savings outweighs that of the transient temperature range. Among the different scenarios, the SSPCM-DGW system shows the greatest effectiveness in Vancouver. On the other hand, in Montreal and Miami, its performance is less favorable due to local weather conditions, leading to increased energy losses. These observations emphasize the importance of considering specific climate factors when designing energy-efficient glazing systems. Moreover, when the SSPCM-DGW system completes its full phase transition, it retains full visual clarity during office hours, making it particularly advantageous for commercial buildings.

For future studies, it is essential to address the current gaps in data related to solid-solid phase change materials (SSPCMs) to fully explore their potential in energy-efficient thermal design applications. A more thorough investigation into their thermophysical and optical properties is required, as existing information remains limited. Additionally, the scarcity of manufacturers producing SSPCMs further restricts experimental research, making it a key area for development.

Future research should prioritize hands-on, experimental studies that focus on the integration of SSPCMs into building envelope systems, where experimental data is notably scarce. Expanding both the availability of data and the production of SSPCMs will be critical in unlocking their full range of applications in the building sector.

### Declaration of conflicting interests

The author(s) declared no potential conflicts of interest with respect to the research, authorship, and/or publication of this article.

### Funding

The author(s) received no financial support for the research, authorship, and/or publication of this article.

### ORCID iDs

Hossein Arasteh  <https://orcid.org/0000-0001-8730-9550>

Wahid Maref  <https://orcid.org/0000-0002-9218-1165>

Hamed H Saber  <https://orcid.org/0000-0003-0197-1645>

### References

- ANSYS Inc. (2021). ANSYS FLUENT Theory Guide, Version 22.1.0, Revision for ANSYS 2022 R1. Canonsburg, PA: ANSYS Inc. Available at: <https://www.ansys.com/> (accessed 22 February 2024).
- Arasteh H, Maref W and Saber HH (2023) Energy and thermal performance analysis of PCM-Incorporated glazing units combined with passive and active techniques: A review study. *Energies* 16(3): 1058.
- ASHRAE (2021) *ASHRAE Handbook of Fundamental, Effective Thermal Resistance of Plane Air Spaces*. ASHRAE.
- Badeche M (2022) Integrated adaptive facades for building energy efficiency and user's thermal comfort. In: Hatti M (ed) *Artificial Intelligence and Heuristics for Smart Energy Efficiency in Smart Cities: Case Study: Tipasa, Algeria*. Springer, 2022, pp.882–888.
- Beck HE, Zimmermann NE, McVicar TR, et al. (2018) Present and future Köppen-Geiger climate classification maps at 1-km resolution. *Scientific data* 5(1): 1–12.
- Berville C, Bode F, Croitoru C, et al. (2024) Enhancing solar façade thermal performance with PCM spheres: A CFD investigation. *Journal of Building Physics* 47(5): 477–495.
- Chen S, Zhou G and Miao C (2019) Green and renewable bio-diesel produce from oil hydrodeoxygenation: Strategies for catalyst development and mechanism. *Renewable and Sustainable Energy Reviews* 101: 568–589.
- Dellagi A, Ayed R, Bouadila S, et al. (2024) Computational and experimental analysis of PCM-infused brick for sustainable heat regulation. *Journal of Building Physics* 48(2): 222–243.

- Dodd T, Orlitzky M and Nelson T (2018) What stalls a renewable energy industry? Industry outlook of the aviation biofuels industry in Australia, Germany, and the USA. *Energy Policy* 123: 92–103.
- Fallahi A, Guldentops G, Tao M, et al. (2017) Review on solid-solid phase change materials for thermal energy storage: Molecular structure and thermal properties. *Applied Thermal Engineering* 127: 1427–1441.
- Gao Y, Zheng Q, Jonsson JC, et al. (2021) Parametric study of solid-solid translucent phase change materials in building windows. *Applied Energy* 301: 117467.
- Goia F, Perino M and Haase M (2012) A numerical model to evaluate the thermal behaviour of PCM glazing system configurations. *Energy and Buildings* 54: 141–153.
- Gowreesunker BL, Stankovic SB, Tassou SA, et al. (2013) Experimental and numerical investigations of the optical and thermal aspects of a PCM-glazed unit. *Energy and Buildings* 61: 239–249.
- Guldentops G, Ardito G, Tao M, et al. (2018) A numerical study of adaptive building enclosure systems using solid–solid phase change materials with variable transparency. *Energy and Buildings* 167: 240–252.
- Jin Q, Long X and Liang R (2022) Numerical analysis on the thermal performance of PCM-integrated thermochromic glazing systems. *Energy and Buildings* 257: 111734.
- Lian M, Liu S, Ding W, et al. (2024) A mechanically robust and optically transparent nanofiber-aerogel-reinforcing polymeric nanocomposite for passive cooling window. *Chemical Engineering Journal* 498: 154973.
- Liang J and Xiang C (2023) A Comprehensive review on design approaches of adaptive photovoltaic Façade. In: *International conference on sustainable buildings and structures towards a carbon neutral future*, 2023, pp. 3–14. Singapore: Springer.
- Loulou R and Labriet M (2008) ETSAP-TIAM: The TIMES integrated assessment model Part I: Model structure. *Computational Management Science* 5: 7–40.
- Ma Y, Li D, Yang R, et al. (2022) Energy and daylighting performance of a building containing an innovative glazing window with solid-solid phase change material and silica aerogel integration. *Energy Conversion and Management* 271: 116341.
- Ministry of Housing and Urban-Rural Development of the People's Republic of China (2016). Code for thermal design of civil buildings. Beijing: China Architecture & Building Press.
- Nur-E-Alam M, Vasiliev M, Yap BK, et al. (2024) Design, fabrication, and physical properties analysis of laminated Low-E coated glass for retrofit window solutions. *Energy and Buildings* 318: 114427.
- Raj CR, Suresh S, Bhavsar RR, et al. (2020) Recent developments in thermo-physical property enhancement and applications of solid solid phase change materials: A review. *Journal of Thermal Analysis and Calorimetry* 139: 3023–3049.
- Saber HH, Alshehri SA and Yarbrough DW (2024a) Innovative airspace reflective tool for different building applications, part I: Tool development. *Science and Technology for the Built Environment*: 30(10), 1–15.
- Saber HH, Alshehri SA and Yarbrough DW (2024b) Innovative airspace reflective tool for different building applications, part II: parametric study. *Science and Technology for the Built Environment* 30(7): 800–821.
- Sun M, Sun H, Wei R, et al. (2024) Energy-efficient smart window based on a thermochromic hydrogel with adjustable critical response temperature and high solar modulation ability. *Gels* 10(8): 494.

- Truong W, Zandi B, Trinh VQ, et al. (2020) Circadian metric–Computation of circadian stimulus using illuminance, correlated colour temperature and colour rendering index. *Building and Environment* 184: 107146.
- Tükel M, Mumcuoğlu K, Arıcı M, et al. (2019) Analysis of fluid flow and heat transfer characteristics in multiple glazing roofs with a special emphasis on the thermal performance. *Applied Thermal Engineering* 148: 694–703.
- Wagiri F, Shih S-G, Harsono K, et al. (2024) Multi-objective optimization of kinetic facade aperture ratios for daylight and solar radiation control. *Journal of Building Physics* 47(4): 355–385.
- Wang P, Liu Z, Zhang L, et al. (2023a) Inversion of extinction coefficient and refractive index of variable transparency solid–solid phase change material based on a hybrid model under real climatic conditions. *Applied Energy* 341: 121098.
- Wang X, Shi X and Jin X (2023b) Study on heat and moisture transfer characteristics of HPCMs. *Journal of Building Physics* 47(1): 121–147.
- Wu S, Sun H, Song J, et al. (2024) Comprehensive analysis on building performance enhancement based on selective split-band modulated adaptive thermochromic windows. *Applied Energy* 372: 123754.
- Xu X, Xie J, Zhang X, et al. (2025) A new validated trnsys module for phase change material-filled multi-glazed windows.
- Yadav S and Hachem-Vermette C (2024) Performance evaluation of semitransparent PV window systems employing periodic thermal model. *Applied Energy* 353: 122076.
- Zhang C, Yang R, Lu Y, et al. (2024) Parametric research on thermal and optical properties of solid-solid phase change material packaged in glazing windows. *Journal of Energy Storage* 83: 110562.
- Zhang Y, Zhang X, Qian T, et al. (2020) Modeling and simulation of a passive variable inertia flywheel for diesel generator. *Energy Reports* 6: 58–68.
- Zhao H and Magoulès F (2012) A review on the prediction of building energy consumption. *Renewable and Sustainable Energy Reviews* 16(6): 3586–3592.

## Appendix

### Notation

A	Area (m <sup>2</sup> )
c <sub>p</sub>	Specific heat (J/kgK)
d	Optical thickness (m)
h	Heat transfer coefficient (W/m <sup>2</sup> K)
h <sub>s</sub>	Sensible enthalpy (J/kg)
H	Enthalpy (J/kg)
ΔH	Latent heat (J/kg)
I	Radiation intensity (W/m <sup>2</sup> )
L	Latent heat of fusion (kJ/kg)
n	refractive index
p	Pressure (Pa)
q <sup>''</sup>	Total heat flux (W/m <sup>2</sup> )
$\vec{r}$	Position vector (m)
s	Sample thickness (path length; m)
$\vec{s}$	Direction vector

$\vec{s}'$	Scattering direction vector
t	Time (s)
T	Temperature (°C)
$T_c$	Phase transition temperature (°C)
$dT_c$	Phase transition temperature range (°C)
v	Velocity (m/s)

### Greek symbols

$\beta$	Transparency fraction
$\mu$	Dynamic viscosity (Pa s)
$\rho$	Density (kg/m <sup>3</sup> )
$\sigma_a$	Absorption coefficient (1/m)
$\sigma_s$	Scattering coefficient (1/m)
$\sigma_e$	Extinction coefficient (1/m)
$\tau$	Transmittance
$\varnothing$	Phase function
$\Omega'$	Solid angle (sr)

### Subscripts

op	Opaque
PCM	Phase change material
ref	Reference
tr	Transparent

### Acronyms

DGW	Double-glazing window
PCM	Phase change material
SLPCM	solid-liquid phase change material
SSPCM	solid-solid phase change material